THE JOURNAL OF BIOLOGICAL CHEMISTRY
Vol. 279, No. 24, Issue of June 11, pp. 25689–25695, 2004
Printed in U.S.A.

The Life Span Determinant p66Shc Localizes to Mitochondria Where It Associates with Mitochondrial Heat Shock Protein 70 and Regulates Trans-membrane Potential*

Received for publication, February 19, 2004, and in revised form, April 9, 2004
Published, JBC Papers in Press, April 12, 2004, DOI 10.1074/jbc.M401844200

Francesca Orsini,[a,b,c,d] Enrica Migliaccio,[a,b,c] Maurizio Moroni,[a,b,e] Cristina Contursi,[a,b,e] Veronica A. Raker,[a] Daniele Piccini,[a,b] Ines Martin-Padura,[a,b,f] Giovanni Pelliccia,[a,b] Mirella Trinei,[a,b] Maria Bono,[b,g] Claudia Puri,[b,g] Carlo Tacchetti,[b,g] Monica Ferrini,[h] Roberta Mannucci,[h] Ildo Nicoletti,[h] Luisa Lanfrancone,[a] Marco Giorgio,[a,b,i] and Pier Giuseppe Pelicci[a,b,j]

From the [a]Department of Experimental Oncology, European Institute of Oncology, Via Ripamonti 435, 20141 Milan, Italy, the [b]Federazione Italiana per la Ricerca sul Cancro (FIRC) Institute of Molecular Oncology, Via Adamello 16, 20139 Milan, Italy, the [g]Department of Experimental Medicine, University of Genova, Via de Toni 14, 16132 Genova, Italy, and the [h]Department of Clinical Experimental Medicine, University of Perugia, Via Brunamonti, 06122 Perugia, Italy

P66Shc regulates life span in mammals and is a critical component of the apoptotic response to oxidative stress. It functions as a downstream target of the tumor suppressor p53 and is indispensable for the ability of oxidative stress-activated p53 to induce apoptosis. The molecular mechanisms underlying the apoptogenic effect of p66Shc are unknown. Here we report the following three findings. (i) The apoptosome can be properly activated *in vitro* in the absence of p66Shc only if purified cytochrome *c* is supplied. (ii) Cytochrome *c* release after oxidative signals is impaired in the absence of p66Shc. (iii) p66Shc induces the collapse of the mitochondrial trans-membrane potential after oxidative stress. Furthermore, we showed that a fraction of cytosolic p66Shc localizes within mitochondria where it forms a complex with mitochondrial Hsp70. Treatment of cells with ultraviolet radiation induced the dissociation of this complex and the release of monomeric p66Shc. We propose that p66Shc regulates the mitochondrial pathway of apoptosis by inducing mitochondrial damage after dissociation from an inhibitory protein complex. Genetic and biochemical evidence suggests that mitochondria regulate life span through their effects on the energetic metabolism (mitochondrial theory of aging). Our data suggest that mitochondrial regulation of apoptosis might also contribute to life span determination.

P66Shc is a splice variant of p52Shc/p46Shc, a cytoplasmic signal transducer involved in the transmission of mitogenic signals from tyrosine kinases to Ras (1). It has the typical domain organization of all members of the Shc family of adaptor proteins (a phosphotyrosine binding domain, a collagen homology 1 (CH1)[1] region, and an Src homology 2 (SH2) domain) and is characterized by a unique amino-terminal region named CH2. P66Shc, however, is not involved in Ras regulation but functions instead in the intracellular pathways that convert oxidative signals into apoptosis (2).

Homozygous deletion of p66Shc in mice (p66Shc−/−) delays senescence and prolongs life span by about one-third, suggesting that p66Shc is a genetic determinant of aging in mammals (3). In aging animal models of both invertebrates and vertebrates, a strong correlation exists between longevity and increased resistance to oxidative stress (4). P66Shc regulates intracellular levels of reactive oxygen species (ROS) (5) and oxidative stress-induced apoptosis (3, 5). Indeed, primary cells isolated from p66Shc−/− mice (hematopoietic precursors, fibroblasts, and endothelial cells) are resistant to oxidative stress-induced apoptosis, whereas overexpression of p66Shc induces apoptosis in the same cellular contexts (5).[2] A critical role of p66Shc in the propagation of apoptogenic stress signals has also been documented *in vivo*. P66Shc−/− mice show markedly reduced signs of tissue damage and apoptosis after limb ischemia,[3] hypercholesterolemic diet (7), diabetes,[2] and challenge with free radicals generating poisons, such as in paraquat intoxication (3).

P66Shc is a downstream target of the tumor suppressor p53. Activated p53 induces p66Shc protein up-regulation by increasing its stability, and overexpression of p53 is unable to induce apoptosis in p66Shc−/− fibroblasts, suggesting that p66Shc regulates p53-dependent apoptosis (5). Genetic evidence, however, indicates that the p53-p66Shc signaling pathway is specifically involved in the propagation of proapoptotic oxidative

* This work was supported by grants from Associazione Italiana Ricerche sul Cancro and Ministero dell'Istruzione dell'Università e della Ricerca. The costs of publication of this article were defrayed in part by the payment of page charges. This article must therefore be hereby marked "*advertisement*" in accordance with 18 U.S.C. Section 1734 solely to indicate this fact.

[c] These authors contributed equally to this work.
[d] Recipient of a Federazione Italiana per la Ricerca sul Cancro (FIRC) fellowship.
[e] Present address: Congenia Srl, Piazzetta Bossi 4, 20100 Milan, Italy.
[f] Recipient of an American-Italian Cancer Foundation (AICF) fellowship.
[i] To whom correspondence may be addressed. Tel.: 39-02-574303240; Fax: 39-02-574303231; E-mail: giorgio@ifom-firct.it.
[j] To whom correspondence may be addressed. Tel.: 39-02-57489868; Fax: 39-02-57489851; E-mail: pgpelicci@ieo.it.

[1] The abbreviations used are: CH1 or CH2, collagen homology region 1 or 2; cyt *c*, cytochrome *c*; ER, endoplasmic reticulum; Hsp, heat shock protein; MEF, mouse embryo fibroblasts; mt, mitochondrial; PDI, protein disulfide isomerase; PT, permeability transition; ROS, reactive oxygen species; SH2, Src homology 2; WB, Western blotting; WT, wild-type.

[2] F. Orsini, E. Migliaccio, M. Moroni, C. Contursi, V. A. Raker, D. Piccini, I. Martin-Padura, G. Pelliccia, M. Trinei, M. Bono, C.Puri, C. Tacchetti, M. Ferrini, R. Mannucci, I. Nicoletti, L. Lanfrancone, M. Giorgio, and P. G. Pelicci, unpublished results.

[3] G. Zaccagnini, F. Martelli, P. Fasaro, A. Magenta, C. Gaetano, A. Di Carlo, M. Biglioloni, M. Giorgio, I. Martin-Padura, P. G. Pelicci, and M. Capogrossi, submitted for publication.

signals, whereas other functions of p53 are not influenced by p66Shc expression (5). The molecular mechanisms through which p66Shc mediates oxidative stress-induced apoptosis are, however, largely unknown.

Indirect evidence suggests that p66Shc induces apoptosis by modulating ROS-induced mitochondrial damage and release of apoptogenic factors. Activated p53 induces a sustained rise in ROS levels that is possibly implicated in the opening of the mitochondrial permeability transition (PT) pore, the release of apoptogenic factors including cytochrome *c* (cyt *c*), and the cytosolic assembly of the apoptosome (5, 8). Expression of p66Shc is required for the ability of p53 to increase ROS and induce cytochrome *c* release (5). Notably, cyclosporin A, a drug that binds to a component of the mitochondrial pore and inhibits its PT and apoptosis, also inhibits p66Shc-mediated apoptosis, suggesting that p66Shc is involved in mitochondrial PT (5). Whether and/or how p66Shc controls mitochondrial PT remains, however, unclear.

EXPERIMENTAL PROCEDURES

Cell Culture, Treatments, and Antibodies—Early passages (3–5) of mouse embryo fibroblasts (MEFs) were treated for 6 h with 2 μM staurosporine for caspase-3 assays and with 800 μM H_2O_2 or 30 J/m^2 UVC (ultraviolet radiation with wavelength of 254 nm) for localization or spectrofluorimetric experiments. The BG-8 mouse monoclonal and the anti-CH2 rabbit antibodies were generated following standard procedures (9). The other antibodies are commercially available. The rabbit polyclonal anti-SH2 (anti-SHC) was from BD Transduction Laboratories, the rabbit polyclonal anti-caspase 3 came from Cell Signaling, the mouse monoclonal anti-mitochondrial heat shock protein 70 (mtHsp70) was purchased from Alexis, the mouse monoclonal anti-CoxIV sub2 was from Molecular Probes, the mouse monoclonal anti-cyt *c* came from PharMingen, the rabbit polyclonal anti-Calnexin was from Santa Cruz Biotechnology, and the rabbit polyclonal anti-PDI was a gift of Dr. R. Sitia. The JC-1 was purchased from Molecular Probe, and cyclosporin A was purchased from Sigma.

Caspase-3 Activation Assays—Fluorescence-activated cell sorting-based determination of cleaved caspase-3 was carried out as follows. MEFs (10^6 cells for each sample) were washed in phosphate-buffered saline, fixed in 1% formaldehyde, permeabilized in 0.1% Triton X-100, and labeled with 1:50 polyclonal anti-caspase-3 antibody. Samples were analyzed by a fluorescence-activated cell sorter (BD Biosciences, with Cell Quest software) using the anti-rabbit fluorescein isothiocyanate-conjugated antibody (Alexis). An *in vitro* assay of caspase-3 was performed as follows. MEFs (10^6 cells for each sample) were lysed in buffer A containing 20 mM HEPES, pH 7.5, 10 mM KCl, 1.5 mM $MgCl_2$, 1 mM EGTA, 1 mM EDTA, 1 mM dithiothreitol, and the protease inhibitor III mixture from Calbiochem (10). The cellular extracts were cleared by centrifugation at 8000 rpm for 10 min and then at 10^5 rpm for 1 h (S-100 fraction). 20 μg of the S-100 fraction was incubated in the absence or presence of 0.25 mg/ml of purified horse cyt *c* (Sigma) at 30 °C for 1 h in buffer A and analyzed by 15% SDS-PAGE and Western blotting (WB).

JC-1 Measurements of the Mitochondrial $\Delta\Psi$—Spectrofluorimetry was carried out as follows. MEFs were incubated with 0.1 μM JC-1 Red in complete culture medium (Molecular Probes) for 30 min and collected by trypsinization. 2×10^6 cells were re-suspended in 1 ml of phosphate buffer and transferred into the fluorometer cuvette. The intensity of fluorescence (red emission of the JC-1 dye) was registered at 590 nm upon excitation at the wavelength of 510 nm and monitored for up to 30 min. Cyclosporin A was added to the cells at 5 μM concentration 45 min before JC-1 staining. Confocal microscopy was carried out as follows. MEFs were seeded on slides, incubated with 0.1 μM JC-1 red (Molecular Probes) for 30 min, washed with phosphate buffer, and analyzed with the MRC 1024 Bio-Rad microscopy equipped with Laser Sharp 2000 software. H_2O_2 was added to a final concentration of 800 μM directly to the chamber of the microscope.

Localization Experiments—Confocal fluorescence microscopy was performed as follows. MEFs were seeded on slides, incubated with Mito Tracker Red (Molecular Probes) in complete culture medium, fixed with 3.7% paraformaldehyde, permeabilized with 0.01% Triton X-100 in phosphate buffer, incubated with the immuno-purified anti-p66Shc antibody or the anti-PDI antibody, and then with the appropriate anti-mouse secondary antibody Cy3 (Amersham Biosciences) or the anti-rabbit or anti-mouse Alexa 488 or Alexa 568 from Molecular Probes. Immunoelectron microscopy was carried out as follows. MEFs were fixed in 2% paraformaldehyde, 0.2% glutaraldehyde in phosphate buffer, scraped, embedded in 12% gelatin with 2.3 M sucrose, mounted on aluminum pins, and frozen in liquid nitrogen. Ultrathin cryo-sections were obtained with a Reichert-Jung Ultra-cut E with a FC4E cryo-attachment and collected on copper-Formvar-carbon-coated grids. Immunogold localization on ultrathin cryo-sections was performed as described previously (11). Sections were immunostained with a rabbit anti-p66 antibody followed by 15-nm protein A-gold and examined with a Zeiss EM 10 and FEI Tecnai 12-G2 electron microscopes. Subcellular fractionation was done as follows. Cells were collected with 10-ml/10-cm dish of cold MTC 0.25 M sucrose buffer (12) using a cell scraper and then broken using a potter. Fresh livers were washed in phosphate buffer and homogenized using a potter in MTC 0.25 M sucrose buffer. Differential centrifugation rounds were then performed to separate nuclei (700 rpm), mitochondria (8000 rpm), the endoplasmic reticulum (15,000 rpm), and the soluble fraction. Submitochondrial fractions were prepared according to established procedures (13) and monitored by polarographic analysis (14).

Chromatographic Methods—Lysates were analyzed by size exclusion chromatography using a fast protein liquid chromatography protein purification system on analytical Superose 6 PC 3.2/30 columns (Amersham Biosciences). The Superose column was eluted at 4 °C with JS buffer (50 mM HEPES, pH 75, 150 mM NaCl, 1.5 mM $MgCl_2$, 5 mM EDTA, 1% glycerol, 1% Triton X-100, 20 mM $Na_4P_2O_7$, pH 7.5, 50 mM NaF, and the protease inhibitor III mixture from Calbiochem) at 40 μl/min, and 50-μl fractions were collected. The column was calibrated with protein standards (Amersham Biosciences) including blue dextran (2000 kDa), thyroglobulin (669 kDa), β-amylase (200 kDa), and bovine serum albumin (66 kDa).

RESULTS

P66Shc Controls Cytochrome c Release from the Mitochondria and the Activation of Cytosolic Caspase-3—Apoptogenic oxidative signals lead to mitochondrial PT and to the release in the cytoplasm of a number of mitochondrial apoptogenic proteins, including cyt *c*. Cytosolic cyt *c* forms a multimeric complex (the apoptosome) with the cytosolic apoptotic protease-activating factor-1 and caspase-9, which leads to cleavage of pro-caspase-3 and activation of the other downstream caspases (10, 15). To investigate whether activation of the apoptosome is regulated by p66Shc, we analyzed the extent of H_2O_2- or staurosporine-induced cleavage of caspase-3 in WT and p66Shc−/− primary MEFs. Staurosporine is an apoptogenic protein kinase *c* antagonist that, like H_2O_2, induces cyt *c* release and caspase-3 cleavage (16). As shown in Fig. 1*A*, H_2O_2 or staurosporine treatment was unable to activate caspase-3 in p66Shc−/− MEFs. Notably, re-expression of p66Shc into p66Shc−/− MEFs restored a normal caspase-3 activation response (Fig. 1*A*).

To investigate which components of the apoptosome or activation steps are defective in p66Shc−/− cells, we analyzed the apoptosome assembly and its functional integrity *in vitro*. Cytosolic fractions (10^5 rpm supernatants) from staurosporine- or H_2O_2-treated cells were analyzed for their ability to activate pro-caspase-3 as determined by WB using specific antibodies against the cleaved caspase-3 fragment. The presence of cytosolic cyt *c* is the only limiting step for the apoptosome activation in this assay, because the addition of purified cyt *c* also induces caspase-3 cleavage in lysates from untreated cells (16). Strikingly, we detected no caspase-3 activation in the lysates of staurosporine-treated p66Shc−/− cells as compared with wild-type MEFs or p66Shc−/− MEFs re-expressing p66Shc (Fig. 1*B*). Notably, the addition of purified cyt *c* to lysates from staurosporine-treated p66Shc−/− MEFs restored caspase-3 activation (Fig. 1*B*). Comparable results were obtained using H_2O_2 or UVC-treated p66Shc−/− MEFs (not shown). These results demonstrate that the apoptosome can be properly activated *in vitro* in the absence of p66Shc only if cyt *c* is supplied, suggesting that optimal concentration of cytosolic cyt *c* is the limiting factor for the activation of the apoptosome in p66Shc−/− cells. Consistently, the concentration of cytosolic

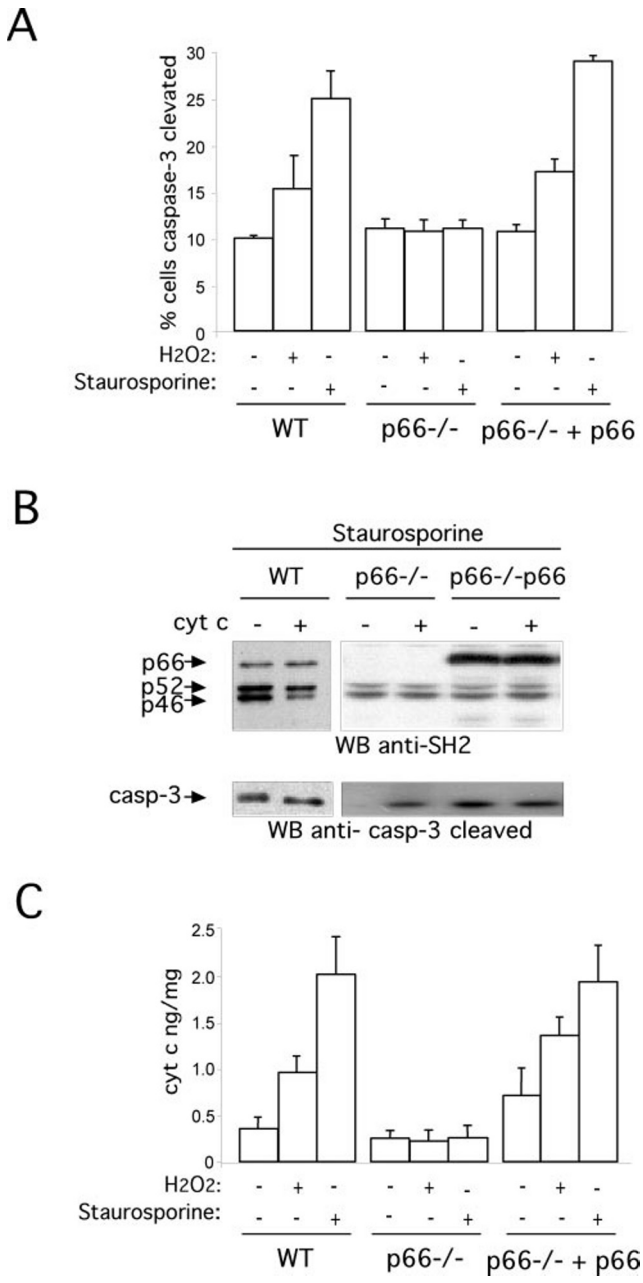

FIG. 1. **P66Shc induces caspase-3 activation, releasing cytochrome *c* from mitochondria.** *A*, caspase-3 activation upon staurosporine treatment of WT and p66Shc−/− MEFs. Flow cytometry analysis was performed using antibodies against cleaved caspase-3 of WT and p66Shc−/− MEFs infected with the vector alone or with the p66Shc cDNA, as indicated, and treated for 6 h with 2 μM staurosporine or 800 μM H_2O_2. *B*, caspase-3 (*casp-3*) cleavage *in vitro* assay with (+) or without (−) the addition of exogenous cyt *c*. WT and p66Shc−/− MEFs, infected with the vector alone or with p66Shc cDNA, were treated for 6 h with 2 μM staurosporine and analyzed for caspase-3 *in vitro* activation as described under "Experimental Procedures." WBs were probed with anti-Shc-SH2 antibodies (*upper panel*) or antibodies specific for the cleaved form of caspase-3 (*lower panel*). *C*, Cyt *c* release. Cytosolic fractions of WT and p66Shc−/− MEFs infected with the vector alone or with the p66Shc cDNA were treated for 6 h with 2 μM staurosporine or 800 μM H_2O_2 and analyzed for cyt *c* concentrations by enzyme-linked immunosorbent assay as described previously (5).

cyt *c* in staurosporine- (Fig. 1*C*), H_2O_2- (Fig. 1*C*), or UVC-treated (not shown) p66Shc−/− MEFs is severely reduced as compared with that of matched control cells (Fig. 1*C*).

P66Shc Is Required for the Collapse of Mitochondrial Transmembrane Potential Induced by Oxidative Stress—A critical event during the mitochondrial PT and the subsequent release

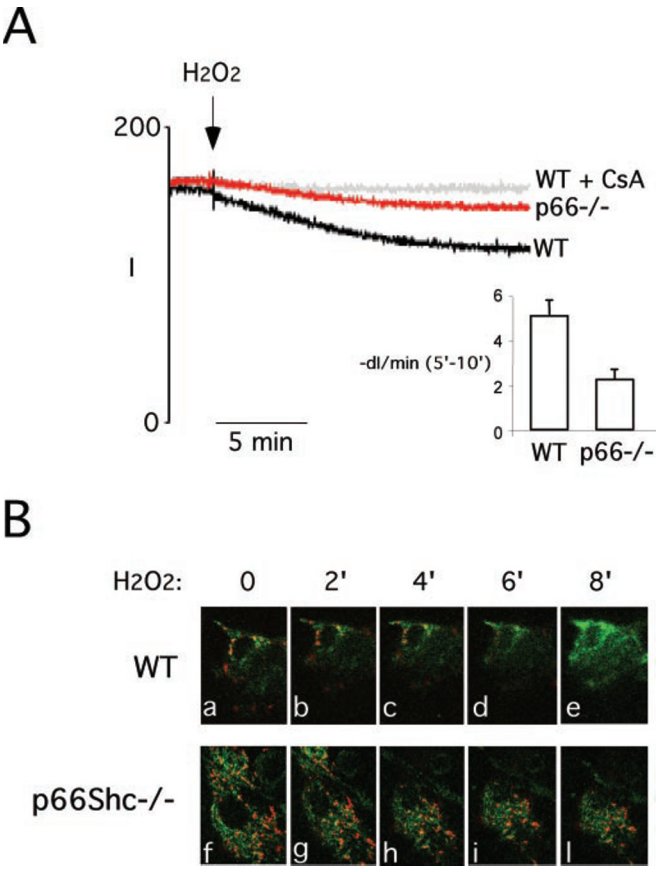

FIG. 2. **P66Shc promotes the collapse of mtΔΨ upon oxidative stress.** *A*, kinetics of JC-1 fluorescence of WT and p66Shc−/− MEFs treated with H_2O_2. The various traces indicate the relative intensity of fluorescence of the high potential emission state of the JC-1 dye, as indicated. All cells were treated with H_2O_2 (at the time point indicated by the *arrow*). WT cells were also treated with cyclosporin A, as indicated. The histogram reports the average slope (calculated for the interval 5–10 min) from four independent experiments. *B*, confocal fluorescence microscopy of WT and p66Shc−/− MEFs stained with the JC-1 and treated with H_2O_2. Images from the same field are collected every 2 min after the addition of H_2O_2; $t = 0$ is set immediately before H_2O_2 addition.

of cyt *c* is the loss of the mitochondrial trans-membrane potential (mtΔΨ) (17, 18). To evaluate the effect of p66Shc on the mtΔΨ, we analyzed the fluorescence emission of WT and p66Shc−/− fibroblasts stained with the specific, potential-sensitive dye JC-1 (19). Because of its positive charge, intracellular JC-1 accumulates within energized mitochondria (high mtΔΨ), where it aggregates because of high local concentrations. During apoptosis, mitochondria become de-energized (low mtΔΨ), and JC-1 is released into the cytoplasm as a monomer (19). The monomeric or aggregated forms of JC-1 can be distinguished by the differences of the emitted light (red at 590 nm or green at 527 nm, respectively) in cells excited with a 510-nm radiation (19). WT and p66Shc−/− MEFs were stained with JC-1 and treated with H_2O_2. JC-1 fluorescence was then analyzed in the entire cell population by spectrofluorometry (Fig. 2*A*) or, at the level of single cells, by confocal fluorescence microscopy (Fig. 2*B*). Prior to H_2O_2 treatment, the JC-1 red emission signals of WT and p66Shc−/− cells were comparable, suggesting that the levels of steady-state mtΔΨ are not influenced significantly by p66Shc (Fig. 2*A*, initial traces). As reported, H_2O_2 treatment of WT cells induced a marked dissipation of the mtΔΨ (see the progressive decrease of fluorescence intensity in Fig. 2*A*, *black line*) and the gradual disappearance of red signals (in Fig. 2*B*, *panels b–e*). In the p66Shc−/− cells the extent of H_2O_2-induced depolarization was, in contrast, reduced significantly (Fig. 2*A*,

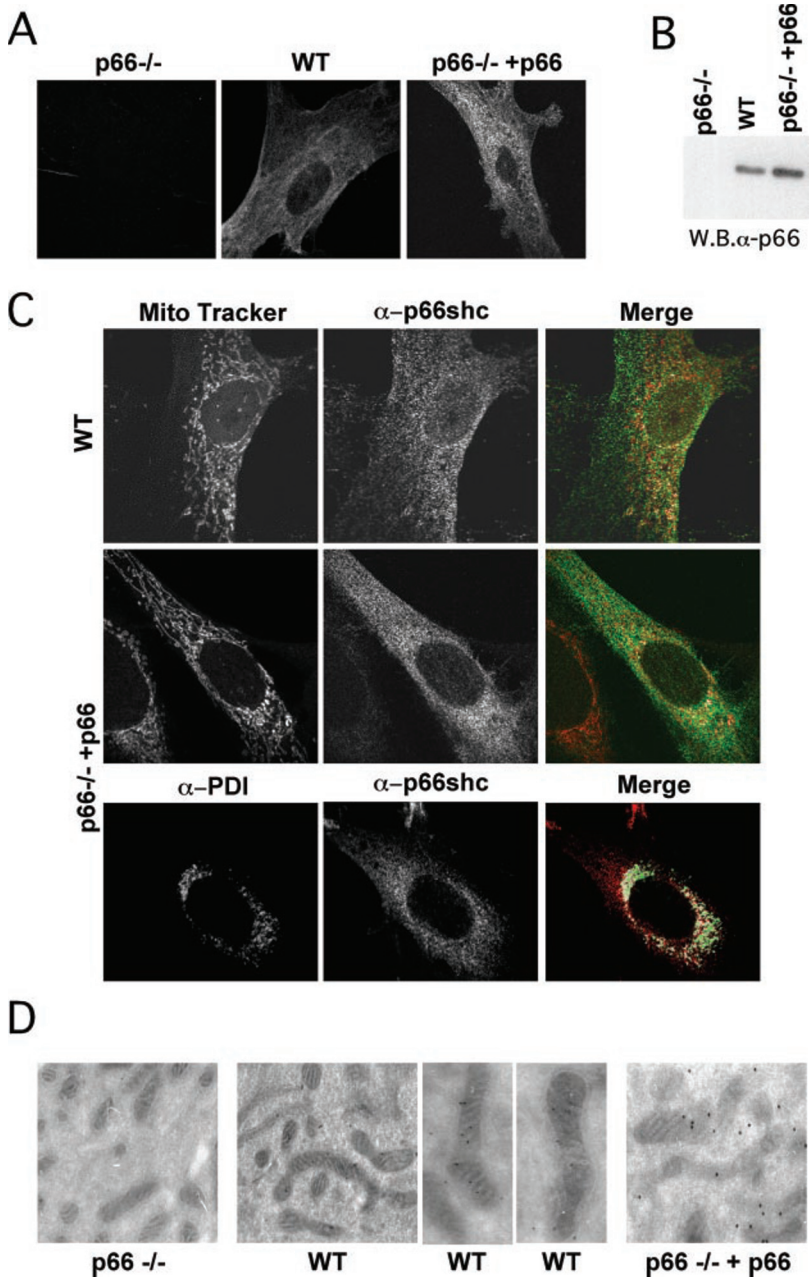

FIG. 3. **Intracellular localization of p66shc *in vivo*.** *A*, specificity controls of the BG-8 anti-p66Shc monoclonal antibody. Confocal immunofluorescence microscopy of WT and p66Shc−/− MEFs and p66Shc−/− MEFs infected with a retroviral vector expressing p66Shc stained with the BG-8 anti-p66Shc monoclonal antibody. *B*, WB analysis of the same cells as in *A* using the BG-8 antibody. *C*, P66Shc compartmentalization *in vivo* by confocal immunofluorescence. WT (*top panels*) and p66Shc−/− MEFs re-expressing p66Shc (*central panels*) were incubated with Mito Tracker Red dye or anti-PDI (*green*) (*lower panels*), decorated with the BG-8 anti-p66Shc antibody, and analyzed by confocal analysis. The *top two panels in the left column* show the signal from the Mito Tracker Red, and the *bottom panel in the left column* shows the anti-PDI staining. *Panels in the central column* show the signal of the anti-p66Shc antibody, and the panels in the *right column* show the merging signal (*in white*). *D*, immunoelectron microscopy on p66Shc. Immunogold localization of p66Shc on ultrathin cryosections of WT MEFs, p66Shc−/− MEFs, and p66Shc−/− MEFs re-expressing p66Shc (*MEFp66−/− +p66*) decorated with a polyclonal (anti-CH2) anti-p66Shc antiserum are shown. No gold particles were found to be associated with either mitochondria or the rough ER in p66Shc−/− MEF, whereas both organelles are labeled in the p66Shc−/− MEF reconstituted with p66 or in the WT MEF.

red line, and 2*B*, *panels g–l*). In particular, the slope of the fluorescence intensity trace measured in the 5–10 min interval after H_2O_2 treatment was reduced by ~50% in the p66Shc−/− cells (see *inset* of Fig. 2*A*). Pre-incubation of WT or p66Shc−/− cells with 5 μM cyclosporin A completely prevented H_2O_2-induced mt$\Delta\Psi$ dissipation, indicating that the target of oxidative damage is either at or upstream of the PT (Fig. 2*A*, *gray line*). It appears, therefore, that p66Shc expression regulates H_2O_2-induced mt$\Delta\Psi$ dissipation.

P66Shc Localizes in Different Intracellular Compartments Including Endoplasmic Reticulum and Mitochondria—Other pro-apoptotic proteins that induce dissipation of the mt$\Delta\Psi$ and cyt *c* release, such as the Bcl-2 like family members Bax, Bad, and Bid, exert their effects directly by associating with the mitochondria (18). Therefore, we investigated the intracellular localization of p66Shc under basal conditions and after oxidative stress by indirect confocal immunofluorescence and immunoelectron microscopy (Fig. 3) and cell fractionation (Fig. 4) experiments.

Confocal immunofluorescence analysis was performed using WT and p66Shc−/− MEFs or p66Shc−/− MEFs re-expressing p66Shc. We generated anti-p66Shc monoclonal antibodies by immunizing p66Shc−/− mice with the p66Shc CH2 region (GST-CH2) expressed in bacteria. The BG8 hybridoma supernatant was selected based on its ability to stain WT but not p66Shc−/− fibroblasts (immunofluorescence analysis; Fig. 3*A*) and to specifically recognize p66Shc polypeptides (Western blotting; Fig. 3*B*). The BG8 staining pattern of WT or p66Shc−/− cells re-expressing p66Shc was cytosolic with a typically punctuated appearance that was most prominent in the perinuclear region (Fig. 3*A*).

To investigate whether a fraction of the cytosolic p66Shc localizes in mitochondria and the endoplasmic reticulum, cells were stained with the Mito Tracker Red dye (a fixable mitochondrial selective probe) or the anti-PDI antibody that recognized the PDI endoplasmic reticulum (ER)-specific protein and with the BG8 antibody. An overlay of Mito Tracker and anti-BG8 staining from untreated WT fibroblasts revealed a partial co-localization (Fig. 3C, *upper panels*). The extent of Mito Tracker/anti-BG8 co-staining increased slightly after treat-

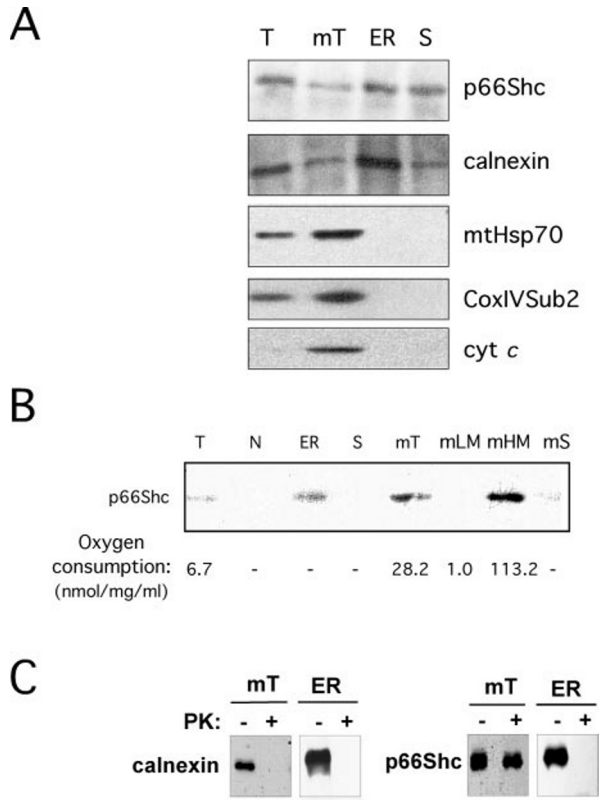

FIG. 4. **Intracellular localization of p66Shc by cellular fractionation.** *A*, Western blot analysis of WT MEFs subcellular fractions using anti-p66Shc, anti-calnexin, anti-PDI anti-mtHp70, anti-CoxIV Sub2, and anti-cyt *c* antibodies. *T*, total extract; *mT*, mitochondria, *S*, cytosol. *B*, Western blot analysis of WT liver sub-cellular fractions using the anti-p66Shc antibodies. Purified liver mitochondria were further fractionated to separate the outer membrane (fraction labeled *mLM*), the inner membrane (fraction labeled *mHM*), and the soluble mitochondrial content (fraction labeled *mS*). *C*, P66Shc is partially protected from proteinase K. Mitochondria- and endoplasmic reticulum-enriched fractions were treated with proteinase K (*PK*) and analyzed by WB with anti-calnexin or anti-p66Shc antibodies, as indicated.

ment with UVC or H_2O_2 (not shown). Image statistical analysis revealed that the percentage of the anti-BG8/Mito Tracker co-stained areas in the untreated fibroblasts was 5.8 ± 0.7%, whereas after UVC the percentage increased up to 11.6 ± 1.6% ($p < 0.01$). Similar results were obtained using p66Shc−/− MEFs re-expressing p66Shc (Fig. 3*C*, *central panels*) or green fluorescent protein-p66Shc (not shown). An overlay of anti-PDI (Fig. 3*C*, *green*) and anti-BG8 staining (Fig. 3*C*, *red*) from p66Shc−/− MEFs re-expressing p66Shc and WT fibroblasts (not shown) revealed a partial co-localization of p66Shc with the PDI ER-specific protein. (Fig. 3*C*, *lower panels*), indicating that p66Shc localized even in the ER.

Similar results were obtained by immunoelectron microscopy using a different anti-p66Shc antibody (a rabbit polyclonal antiserum against the CH2 region of p66Shc). This antibody stained WT and p66Shc−/− MEFs re-expressing p66Shc but not the p66Shc−/− cells (Fig. 3*D*). Quantitative analysis of electron microscopy images revealed that ~44% of the total score of p66Shc signals lies within the mitochondria and 24% in the ER (Table 1).

To obtain an independent confirmation of the mitochondrial localization of p66Shc, we analyzed the expression of p66Shc within various subcellular fractions obtained by differential centrifugations of cellular lysates and mouse liver or lung homogenates (12). The enrichment for mitochondria in the various fractions was monitored by measuring oxygen consumption (using a Clark-type electrode; polarographic analysis) or by

TABLE I
Morphometry on p66Shc immunogold immunoelectron microscopy localization

Shown are the number of gold particles associated with mitochondria, rough endoplasmic reticulum (RER), and other organelles. Data refer to the number of gold particles counted on 10 cell profiles by immunoelectron microscopy analysis. The percentage of the gold distribution in each compartment compared to the total gold particles counted is also indicated. Data refer to one representative experiment of three performed.

	Mitochondria	RER	Other	Total
Gold particles	159	87	112	358
Percentage (%)	44	24	32	100

Western blotting using antibodies against different mitochondrial proteins, including cyt *c*, the subunit 2 of the cyt *c* oxidase (COX IV), and mtHsp70. The ER fraction was monitored using antibodies against ER-specific proteins, calnexin, and PDI. Representative experiments using subcellular fractions from WT MEFs or mouse liver homogenates are shown in Fig. 4, *A* and *B*, respectively. Consistently, we detected p66Shc in the soluble, mitochondrial, and ER fractions, although with different reciprocal distributions when comparing different samples. Notably, in the liver fractions the presence of p66Shc correlated significantly with the highest respiratory activity (Fig. 4*B*). To preliminarily map p66Shc expression within mitochondria, purified liver mitochondria were further fractionated to separate the outer (Fig. 4*B*, *mLM*) and inner (Fig. 4*B*, *mHM*) membranes and the soluble content (Fig. 4*B*, *mS*). P66Shc was retained with the sub-mitochondrial fraction enriched for the inner membrane, which retains the highest respiratory activity (Fig. 4*B*). To confirm that p66Shc localizes within mitochondria, the mitochondrial and the ER-containing fractions were treated with proteinase K, which can digest only those proteins that are not protected by closed phospholipidic bilayers (20). As expected, proteinase K degraded calnexin in the ER fraction (Fig. 4*C*; the calnexin is a ER-associated protein whose presence in the mitochondrial fraction is due to contaminating ER, as shown in Fig. 4*A*). Notably, the p66Shc of the ER fraction, but not that of the mitochondrial fraction, was degraded by proteinase K (Fig. 4*C*), suggesting that some of the cytosolic p66Shc is associated with the ER membranes and confirming that mitochondrial p66Shc is mainly localized within these organelles.

UVC Treatment Induces the Release of Mitochondrial p66Shc from High Molecular Mass Complexes—The localization experiments described above indicate that a fraction of p66Shc localizes within mitochondria under basal conditions and that apoptogenic oxidative signals (H_2O_2 or UV) induce only a modest (~50%) accumulation of mitochondrial p66Shc. To investigate whether oxidative stress induces modifications of mitochondrial p66Shc, we investigated the extent of p66Shc association within multimolecular complexes by size exclusion chromatography before and after stress treatment.

Mitochondrial fractions (Fig. 5*A*, *upper right panel*) from WT MEFs, prior and after UVC treatment, were analyzed by fast protein liquid chromatography using a Superose-6 size exclusion chromatographic column, and the eluted fractions (fractions 10–22; see chromatogram in Fig. 5*A*) were analyzed by Western blotting using antibodies against p66Shc and mtHsp70. In the mitochondrial fractions from untreated MEFs, p66Shc eluted within the high molecular mass gel filtration fractions with a peak in the fractions that had an apparent molecular mass of 670 kDa (Fig. 5*A*, *lower panel*). Strikingly, 10 min of UVC treatment of WT MEFs provoked the complete disappearance of p66Shc from the high molecular mass size exclusion chromatography fractions and its appearance within

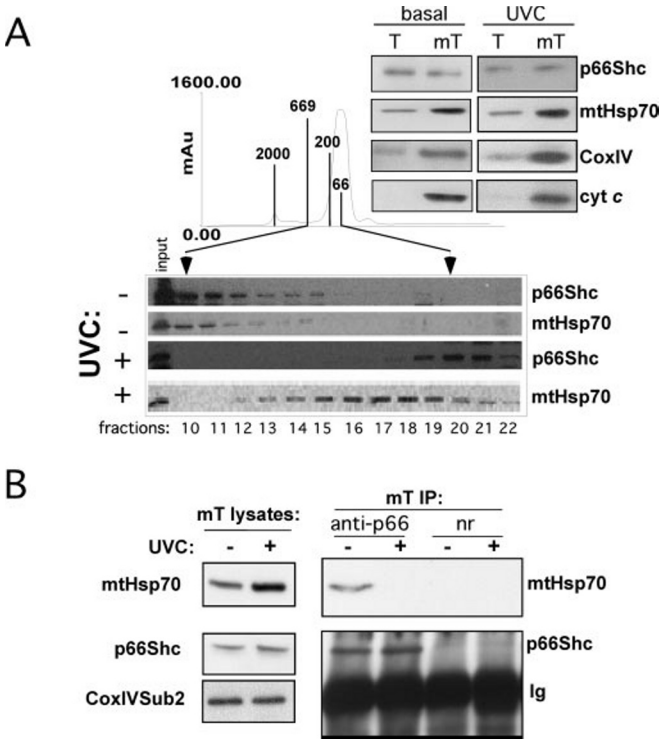

FIG. 5. **Gel filtration and co-immunoprecipitation analysis of p66Shc and mtHsp70 in mitochondrial-enriched fractions.** *A*, gel filtration of mitochondrial-enriched fractions from untreated and UVC-treated WT MEFs. MT fractions from untreated and UVC-treated WT MEFs were analyzed for p66Shc expression and the extent of mitochondrial enrichment (as compared with total lysates, designated *T*) by WB using anti-p66Shc, mtHsp70, CoxIV Sub2, and cyt *c* (*upper panels*). Separation of the references are indicated by *vertical lines* on the chromatogram (2000 kDa = blue dextran; 669 kDa = thyroglobulin; 200 kDa = β-amylase; 66 kDa = albumin). Eluted fractions (from 10 to 22) were analyzed by WB using anti-p66Shc and anti-mtHsp70 antibodies, as indicated. *B*, co-immunoprecipitation of p66Shc and mtHsp70 from mitochondrial-enriched fractions from untreated and UVC-treated WT MEFs. Western blot of total lysates from mitochondrial fractions of untreated and UVC-treated WT MEFs were probed with anti-mtHsp70, anti-p66Shc, and the anti-Cox IV Sub2 antibodies (*left panels*). The same lysates were immunoprecipitated with anti-p66Shc or unrelated (*nr*) antibodies (*right panels*) and analyzed by Western blotting using anti-mtHsp70 (*upper panel*) or anti-p66Shc (*lower panel*) antibodies.

the low molecular mass fractions with a peak of ~66 kDa (Fig. 5*A*). These data suggest that mitochondrial p66Shc exists within high molecular mass complexes under basal conditions and that it becomes monomeric after oxidative stress treatment.

Mitochondrial p66Shc Forms a Stable Complex with mtHsp70 That Is Released after UVC Treatment—Western blotting analysis of the same mitochondrial size exclusion chromatography fractions revealed a behavior of mtHsp70 similar to that of p66Shc. In untreated cells, mtHsp70 eluted in the same high molecular mass fractions of p66Shc (peak around 669 kDa), whereas after UVC treatment, it was detected within lower molecular mass fractions with a peak of ~150–200 kDa (Fig 5*A*, *second* and *fourth row of the lower panel*). To investigate whether p66Shc and mtHsp70 form a stable complex, we performed co-immunoprecipitation experiments using mitochondrial fractions from untreated and UVC-treated WT MEFs. Mitochondria were purified from untreated or treated (by UVC for 10 min) WT MEFs. Western blotting analysis of total mitochondrial lysates showed a slight increase of p66Shc expression following UVC treatment, which is consistent with the immunofluorescence results, and a slight increase of mtHsp70 expression as well (Fig. 5*B*; *left panels*). Anti-Hsp70 Western blotting of anti-p66Shc immunoprecipitates from the same lysates revealed the existence of a stable p66Shc-Hsp70 complex in the untreated cells (Fig. 5*B*, *right panels*). The same, however, was not detected in mitochondrial lysates from UVC-treated MEFs (Fig. 5*B*, *right panels*). It appears, therefore, that mitochondrial p66Shc forms a stable complex with mtHsp70, which is released after UVC treatment.

DISCUSSION

P66Shc mediates oxidative stress-induced apoptosis. The underlying molecular mechanisms, however, remain unknown. We reported here that a fraction of p66Shc localizes within mitochondria and is part of a high molecular mass complex that also contains mtHsp70. After the propagation of apoptogenic oxidative stress signals, the fraction of mitochondrial p66Shc increases slightly and dissociates from mtHsp70. Heat shock proteins are known negative regulators of apoptosis (21). In particular, mtHsp70 (also known as Mortalin/Mot-2/GRP75/PBP74) is a member of the Hsp70 family of chaperons, which is involved in the regulation of cell senescence and immortalization. Among others, mtHsp70 associates with p53 (23) and voltage-dependent anion channel 1 (24), a putative component of the PT pore. Treatment with H_2O_2 induces up-regulation of mtHsp70, which is thought to protect mitochondria from oxidative stress (25). Depletion of mtHsp70 sensitizes cells to ionizing radiations, whereas its over-expression inhibits apoptosis and delays the senescence of primary cells (22, 26, 27). It appears, therefore, that mtHsp70 acts in the mitochondria to prevent oxidative stress-induced mitochondrial damage. It is tempting to speculate that one of the targets of mtHsp70 is mitochondrial p66Shc, whose apoptogenic function might be inhibited when complexed to Hsp70. Notably, transgenic worms that constitutively overexpress the Hsp70 homolog show a life span extension, suggesting that Hsp70 is indeed a genetic determinant of life span in *Caenorhabditis* (27).

The other known biochemical activity of p66Shc is the regulation of ROS metabolism. P66Shc−/− cells have reduced concentrations of steady-state ROS and reduced ROS up-regulation during p53-induced apoptosis, suggesting that p66Shc regulates ROS metabolism (5, 8).[3] Because oxygen radicals are potent inducers of the mitochondrial PT due to their direct effect on the PT pore (28), p66Shc might induce mitochondrial PT by increasing mitochondrial ROS levels. Accordingly, regulation of mitochondrial ROS levels would be the primary effect of mitochondrial p66Shc. Alternatively, ROS could be generated as the consequence of the mitochondrial damage provoked by p66Shc through ROS-independent mechanisms. In either cases, activation of mitochondrial p66Shc would result into the collapse of the $mt\Delta\Psi$.

How p66Shc enters in the mitochondria and injures mitochondrial integrity is, however, unknown. We have recently demonstrated that another Shc isoform, p46Shc, localizes almost exclusively to mitochondria (29). Through deletion-mapping experiments we showed that targeting of p46Shc to mitochondria is mediated by its first 32 amino acids, which behave as a bona fide mitochondrial targeting sequence. This mitochondrial signal peptide is also present in the p66Shc protein. However, differently than p46Shc, p66Shc is not actively imported into mitochondria in an *in vitro* import assay (29). This is consistent with the finding that the N-terminal location of this signal peptide is critical for its function and that the same sequence is more internally located in p66Shc (29). P66Shc has been recently identified within mitochondrial associated membranes obtained from a mitochondrial-enriched fraction.[4] The mitochondrial associated membrane fraction includes the ER

[4] R. Rizzuto, personal communication.

membranes intimately connected to the mitochondria and is characterized by the presence of components of the ER mitochondrial network, namely the inositol 1,4,5-trisphosphate-sensitive Ca^{2+} release channel (30). Therefore, p66Shc might enter the mitochondria through a mechanism involving ER mitochondria contacts.

The mitochondrial theory of aging proposes that an accumulation of damage to mitochondria and mitochondrial DNA leads to aging. Indeed, age-related impairment in the respiratory enzymes not only decreases ATP synthesis but also enhances production of ROS, which is thought to be responsible for the increased rates of mitochondrial DNA mutations and mitochondrial oxidation damage that are observed in the aged tissues (6). Our data indicate that p66Shc regulates apoptosis by acting at the level of mitochondria, possibly through the permeability transition pore, thereby suggesting that mitochondrial regulation of apoptosis might also contribute to life span determination.

Acknowledgments—We are grateful to Paolo Bernardi, Rosario Rizzuto, and Saverio Minucci for discussions and critical reading of the manuscript and to Pietro Transidico for excellent technical assistance with the confocal microscope.

REFERENCES

1. Pelicci, G., Lanfrancone, L., Grignani, F., McGlade, J., Cavallo, F., Forni, G., Nicoletti, I., Grignani, F., Pawson, T., and Pelicci, P. G. (1992) *Cell* **70,** 93–104
2. Migliaccio, E., Mele, S., Salcini, A. E., Pelicci, G., Lai, K. M., Superti-Furga, G., Pawson, T., Di Fiore, P. P., Lanfrancone, L., and Pelicci, P. G. (1997) *EMBO J.* **16,** 706–716
3. Migliaccio, E., Giorgio, M., Mele, S., Pelicci, G., Reboldi, P., Pandolfi, P. P., Lanfrancone, L., and Pelicci, P. G. (1999) *Nature* **402,** 309–313
4. Guarente, L., and Kenyon, C. (2000) *Nature* **408,** 255–262
5. Trinei, M., Giorgio, M., Cicalese, A., Barozzi, S., Ventura, A., Migliaccio, E., Milia, E., Padura, I. M., Raker, V. A., Maccarana, M., Petronilli, V., Minucci, S., Bernardi, P., Lanfrancone, L., and Pelicci, P. G. (2002) *Oncogene* **21,** 3872–3878
6. Sastre, J., Pallardo, F. V., and Vina, J. (2003) *Free Radic. Biol. Med.* **35,** 1–8
7. Napoli, C., Martin-Padura, I., De Nigris, F., Giorgio, M., Mansueto, G., Somma, P., Condorelli, M., Sica, G., De Rosa, G., and Pelicci, P. G. (2003) *Proc. Natl. Acad. Sci. U. S. A.* **100,** 2112–2116
8. Nemoto, S., and Finkel, T. (2002) *Science* **295,** 2450–2452
9. Harlow, E., and Lane, D. (1988) *Antibodies: A Laboratory Manual*, Cold Spring Harbor Laboratory Press, Cold Spring Harbor, NY
10. Liu, X., Kim, C. N., Yang, J., Jemmerson, R., and Wang, X. (1996) *Cell* **86,** 147–157
11. Schiaffino M. V., D'Addio M., Alloni A., Baschirotto C., Valetti C., Cortese K., Puri, C., Bassi, M. T., Colla, C., Luca, M., Tacchetti, C., and Ballabio A. (1999) *Nat. Genet.* **23,** 108–112
12. Pon, L. A., and Schon, E. A. (eds) (2001) *Mitochondria: Methods in Cell Biology*, Vol. 65, Academic Press, New York
13. Nicolli, A., Basso, E., Petronilli, V., Wenger, R. M., and Bernardi, P. (1996) *J. Biol. Chem.* **271,** 185–192
14. Brown, G. C., and Cooper, C. E. (1995) *Bioenergetics: A Practical Approach*, IRL Press, Oxford
15. Zou, H., Li, Y., Liu, X., and Wang, X. (1999) *J. Biol. Chem.* **274,** 11549–11556
16. Li, K., Li, Y., Shelton, J. M., Richardson, J. A., Spencer, E., Chen, Z. J., Wang, X., and Sanders, W. R. (2000) *Cell* **101,** 389–399
17. Marchetti, P., Castedo, M., Susin, S. A., Zamzami, N., Hirsh, T., Macho, A., Harffner, A., Hirsh, F., Geuskens, M., and Kroemer, G. (1995) *J. Exp. Med.* **184,** 1155–1160
18. Wang, X. (2001) *Gen. Dev.* **15,** 2922–2933
19. Reers, M., Smiley, S. T., Mottola-Hartshorn, C., Chen, A., Lin, M., and Chen, L. B. (1995) *Methods Enzymol.* **260,** 406–417
20. Gonzalez-Baro, M. R., Granger, D. A., and Coleman, R. A. (2001) *J. Biol. Chem.* **276,** 43182–43188
21. Bruey, J. M., Ducasse, C., Bonniaud, P., Ravagnan, L., Susin, S. A., Diaz-Latoud, C., Gurbuxani, S., Arrigo, A. P., Kroemer, G., Solary, E., and Garrido, C. (2000) *Nat. Cell Biol.* **2,** 645–652
22. Wadhwa, R., Yaguchi, T., Hasan, M. K., Mitsui, Y., Reddel, R. R., and Kaul, S. C. (2002) *Exp. Cell Res.* **274,** 246–253
23. Schwarzer, C., Barnikol-Watanabe, S., Thinnes, F. P., and Hilschmann, N. (2002) *Int. J. Biochem. Cell Biol.* **34,** 1059–1070
24. Mitsumoto, A., Takeuchi, A., Okawa, K., and Nakagawa, Y. (2002) *Free Radic. Biol. Med.* **32,** 22–37
25. Sadekova, S., Lehnert, S., and Chow, T. Y. (1997) *Int. J. Radiat. Biol.* **72,** 653–660
26. Kaul, S. C., Yaguchi, T., Taira, K., Reddel, R. R., and Wadhwa, R. (2003) *Exp. Cell Res.* **286,** 96–101
27. Yokoyama, K., Fukumoto, K., Murakami, T., Harada, S., Hosono, R., Wadhwa, R., Mitsui, Y., and Ohkuma, S. (2002) *FEBS Lett.* **516,** 53–57
28. Bernardi, P. (1999) *Physiol. Rev.* **79,** 1127–1155
29. Ventura, A., Maccarana, M., Raker, V. A., and Pelicci, P. G. (2004) *J. Biol. Chem.* **279,** 2299–2306
30. Rizzuto, R., Pinton, P., Carrington, W., Fay, F. S., Fogarty, K. E., Lifshitz, L. M., Tuft, R. A., and Pozzan, T. (1998) *Science* **280,** 1763–1766